

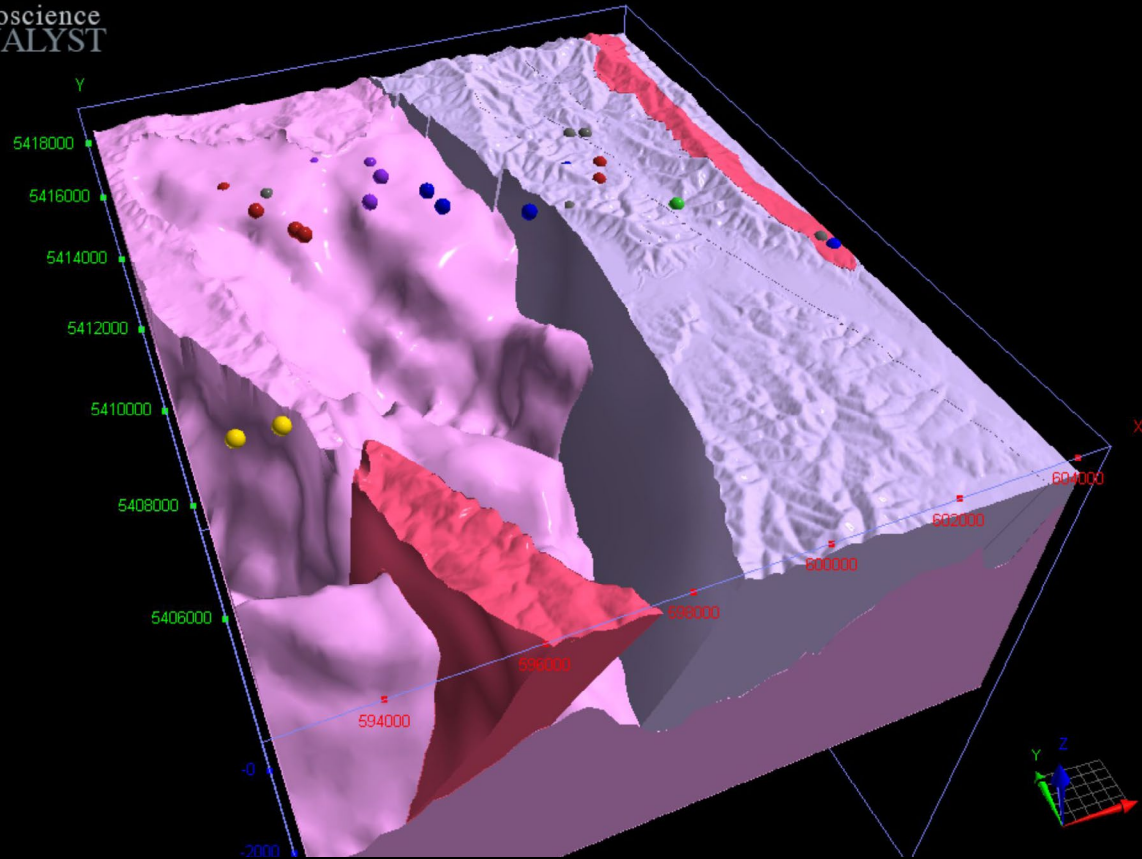


# Scamander 3D Model

Author: D. Bombardieri and M. Duffett  
Date: 15/12/2021  
Email: [info@mrt.tas.gov.au](mailto:info@mrt.tas.gov.au)  
Website: [www.mrt.tas.gov.au](http://www.mrt.tas.gov.au)

REPORT No.: UR2021\_37

Geoscience  
ANALYST



## Geological Survey Explanatory Notes





Mineral Resources Tasmania  
Department of State Growth

# Scamander 3D Model: Explanatory Notes

*by D. Bombardieri and M. Duffett*

Cover: Views of the Scamander 3D Model.

While every care has been taken in the preparation of this report, no warranty is given as to the correctness of the information and no liability is accepted for any statement or opinion or for any error or omission. No reader should act or fail to act on the basis of any material contained herein. Readers should consult professional advisers. As a result the Crown in Right of the State of Tasmania and its employees, contractors and agents expressly disclaim all and any liability (including all liability from or attributable to any negligent or wrongful act or omission) to any persons whatsoever in respect of anything done or omitted to be done by any such person in reliance whether in whole or in part upon any of the material in this report. Crown Copyright reserved.

## ***Abstract***

*Mineral Resources Tasmania (MRT) has developed a high-resolution 3D model of the Scamander mineral province, northeast Tasmania. The geological model expresses a structural synthesis based on mapping and multiple cross-sections developed by MRT staff. The model is constrained by 3D geophysical modelling using MRT's gravity and magnetic data coupled with drilling and rock physical property databases. Statistically generated sensitivity characterisation is incorporated into 3D model products as a step towards estimating confidence in the spatial variability of geological objects at depth. Joint inversion results show that calculated gravity and magnetic responses are in good agreement with observations. A product of sensitivity modelling is a new granite surface, which is significantly more detailed when compared to previous versions. This result supports the hypothesis of granite-derived fluids as the most likely source of metals, with the temperature of the fluid and distance from granite controlling the mineralogy of the deposits in the Scamander Mineral Field.*

*The fusion of geological and geophysical information with measures of model sensitivity is a significantly more sophisticated addition to MRT's suite of public pre-competitive geoscience products, and should further reduce exploration risk.*

## Scamander 3D Model: Explanatory Notes

by D. Bombardieri and M. Duffett  
*Geological Survey Branch - Mineral Resources Tasmania*

### CONTENTS

|  |   |
|--|---|
| 1.0 DATA DELIVERY AND VISUALISATION .....            | 4 |
| 2.0 MODEL CONTENTS.....                              | 4 |
| 2.1 Cross Sections.....                              | 4 |
| 2.2 Deposits .....                                   | 4 |
| 2.3 Drill holes .....                                | 4 |
| 2.4 Granitoid models .....                           | 4 |
| 2012 granite surface .....                           | 4 |
| 2021 granite surface .....                           | 4 |
| 2.5 Input - 3D Geological Modelling .....            | 4 |
| Geology Reference Model – Volumes .....              | 4 |
| Faults .....   | 4 |
| 2.6 Output - 3D Geophysical Modelling .....          | 4 |
| Calculated datasets .....                            | 4 |
| Observed datasets.....                               | 4 |
| Sensitivity statistics.....                          | 4 |
| Vector overlays.....                                 | 5 |
| Digital elevation model (DEM) .....                  | 5 |
| 25K Geology .....                                    | 5 |
| 3.0 GEOPHYSICAL MODELLING METHODOLOGY - SUMMARY..... | 5 |
| 4.0 REFERENCES .....                                 | 7 |

## 1.0 DATA DELIVERY AND VISUALISATION

The model is being distributed primarily as a Geoscience ANALYST project and is described here as such. Geoscience ANALYST is visualisation and communication software for GoCAD® 3D models, made freely available by Mira Geoscience (<http://www.mirageoscience.com/>). All major components of the 3D modelling process from geological cross sections to geophysical inversion results are available in their original formats. Metadata for these contents is given below.

All spatial objects within the model are referenced to the Map Grid of Australia zone 55 and the Australian Height Datum.

## 2.0 MODEL CONTENTS

### 2.1 Cross Sections

The large-scale structure of the area is represented by the three interpretive cross sections. These sections were compiled using field and geophysical data combined with SpheriStat™ profiles and illustrate the structural differences either side of a major northeast to southwest-trending strike-slip (Orieco Fault) (Worthing and Woolward, 2010).

### 2.2 Deposits

Scamander mineral field deposit locations were extracted from the MRT mineral occurrence database.

### 2.3 Drill holes

Collar and hole geometry for the 33 open file drillhole in the model area are from MRT's drilling database. Available online: URL [https://www.mrt.tas.gov.au/products/database\\_searches/drill\\_holes](https://www.mrt.tas.gov.au/products/database_searches/drill_holes)

### 2.4 Granitoid models

Granitoid models indicating evolution in understanding of 3D geometry of regional Devonian granitoid intrusions. The surfaces are thus an undifferentiated amalgamation of all Blue Tier and Scottsdale Batholith plutons.

- **2012 granite surface:** Interpolated surface generated from geometry inversion (GoCAD™). Modified after Leaman, 2012.
- **2021 granite surface:** Interpolated probability threshold surface developed in this study (see below).

### 2.5 Input - 3D Geological Modelling

- **Geology Reference Model – Volumes:** Geological units in the reference model, include the Lone Star Siltstone, Sideling Sandstone and Scamander Formation, which represent sub-units of the Mathinna Supergroup and correspond to stratigraphic units

identified in 1:25,000 scale mapping. The Mathinna Supergroup was intruded by large volumes of granitic and granodioritic magma over a period of about 23 Ma from about 377 to 400 Ma (Black et al., 2005). These intrusives are represented in the model as the Devonian Granite (i.e., Blue Tier Batholith), and Granodiorite (i.e., Catos Creek and Scamander Tier Dykes) respectively.

- **Faults:** Surfaces are interpreted from surface mapping and cross sections. Identified as either normal or thrust.

### 2.6 Output - 3D Geophysical Modelling

- **Calculated datasets**
  - Calculated gravity response: 2D grid of the gravity response (mGal) computed from final model iteration of the cooperative inversion.
  - Calculated TMI response: 2D grid of the magnetic response (nT) computed from final model iteration of the joint inversion
  - Residual gravity response: 2D grid of the residual gravity response (nT) computed from subtracting the final model iteration from the observed gravity response.
  - Residual TMI response: 2D grid of the residual magnetic response (nT) computed from subtracting the final model iteration from the observed TMI response.
- **Observed datasets**
  - Observed TMI response: 2D grid of total magnetic intensity, from MRT data (200 metre line spacing).
  - Observed gravity response: 2D grid of isostatic residual complete Bouguer gravity anomaly (mGal).
- **Sensitivity statistics:** 3D sectional representation of summary statistics for 1.4 billion inversion iterations. The suite of statistical sensitivity products made available for model interrogation include the following
  - Entropy, records the volatility of a particular voxel during the inversion. A value of zero indicates low volatility and 1 high volatility.
  - Mean density, derived from the accumulated accepted inversion proposals/models
  - Mean susceptibility, derived from the accumulated accepted inversion proposals/models
  - Probability of individual unit lithology, the probability of finding an individual geological unit with the whole model space which varies between 0% (black voxels) and 100% (white voxels).

- **Vector overlays**
  - 250kline geology and faults: a vector file of lithological boundaries and faults, extracted from MRT's 1:250,000 seamless geological map coverage
  - Tenements: vector file of exploration licence areas, extracted from MRT register (Dec 11 2021)
- **Digital elevation model (DEM):** Surface topography of the Scamander model area. Extracted from MRT's statewide digital elevation model and resampled to 100 metre cells.
- **25K Geology** – image extracted from published MRT 1:25,000 mapping

### 3.0 GEOPHYSICAL MODELLING METHODOLOGY - SUMMARY

Mineral Resources Tasmania (MRT) has developed a geophysical inversion workflow to image complex terranes in 3D (see Bombardieri et al 2020, and Bombardieri et al., 2021).

The Scamander area, located in northeast Tasmania, is an example of a zoned mineral field, with mineralogy interpreted as a function of distance from the interpreted source granite intrusion (Groves, 1972). W-Mo occurs adjacent to outcropping granite in the NE extending south-eastwards through Sn (Great Pyramid) and Cu (Orieco) to Ag-Pb-Zn near the coast. Zonation is hypothesized to reflect a gently dipping subsurface extension of the granite beneath the mineral field (Ruxton et al., 1984) which is broadly confirmed by gravity modeling (Duffett, 1992). The country rock intruded by the granite is the upper Mathinna Supergroup, comprising correlates of the Siluro-Devonian, Lone Star Siltstone and Sideling sandstone and the Devonian Scamander Formation.

The Scamander 3D model was constructed in GoCAD® Mira Geoscience as a synthesis of all previous work and relied heavily on the structural interpretation by MRT staff as part of the 2005 – 2009 TasExplore initiative. The model dimensions are 15 x 12 km and a depth of 12 km encompassing the Scamander mineral field.

Model elements include, Silurian-Devonian Mathinna Supergroup sediments, Devonian intrusives and an undifferentiated basement lithology. The level of geological detail incorporated into the model is dictated by likely bulk physical property contrast as well as tectonic, stratigraphic, and practical modelling considerations.

The workflow incorporates geological information in the form of cross-sections representing structural interpretations and petrophysical data in the form of unit

rock property density and susceptibility measurements. A “reference model” comprising surfaces representing the various lithologies and fault architecture is first constructed. This model is then discretised in preparation for forward and inverse modelling using GoCAD's potential field module (VPmg code; Fullagar et al., 2008). Geological information (cross sections) is used to constrain geophysical inversion and reduce uncertainty. The 3D model derived to this point (which itself has undergone deterministic geophysical validation) is a ‘best estimate’ synthesis that is consistent with observed gravity and magnetic data. However, as is well recognised for potential field data, this solution is not unique.

3D GeoModellerTM is employed to explore the range of similarly plausible possible models. The stochastic exploration algorithm takes a Monte Carlo approach, generating a sequence of linked models starting with the reference model making small “random” changes to the lithological boundaries and physical properties. Model sensitivity is quantified by measuring the evolution of geological bodies via changes to their volume. The commonality and shape ratio probability functions are the two methods used to perform geological tests on proposed cell perturbation or volume change. The commonality constraint aims to preserve a cell's original lithology by limiting the degree to which it can vary. This constraint is controlled by a Weibull distribution with a scale parameter ranging from 0.5 (loose) to 0.05 (tight). In contrast, the shape ratio aims to preserve the shape of the original lithology. It is defined as the shape of the lithological unit in the proposed model divided by the shape of the lithological unit in the reference model. The constraint is controlled by a log normal distribution with the scale parameter (i.e., standard deviation) ranging from 0.5 (loose) to 0.05 (tight) (McInerney et al., 2013).

For the Scamander inversion, scale parameters (0.5) were used for geological boundary tests on Mathinna Supergroup, granodiorite and basement lithologies. In contrast, a tighter constraint (0.05) was used for the Devonian Granite to account for density variations within the dyke portion of the intrusive. Loose constraints have an impact on the rate of convergence for the joint inversion process by increasing the number of geological acceptances. This in turn increases the number of geophysical acceptances (Bombardieri et al. 2020). For each iteration, if the geological boundary change is accepted then the geophysical response of the adjusted model (constrained by petrophysical information enforced by statistical distribution laws) is calculated. This model response is assessed, and the proposal is accepted or rejected depending on whether the misfit is improved or maintained below an acceptable threshold.

Another parameter used in the inversion is the probability of property change parameter which is set as a ratio. In default mode the ratio is 50/50 meaning there's an equal split between changes made to lithological boundaries and changes to petrophysical properties of the unit. For the Scamander inversion run, a ratio of 60/40 was used with the goal of controlling acceptable levels of geological-boundary variation (Bombardieri et al., 2020).

Upon completion of the cooperative inversion run GeoModellerTM carries out an analysis of the ensemble of models that reproduced the observations to an acceptable degree (Bombardieri et al., 2020). Approximately 117 million acceptable models were generated for sensitivity analysis. Of these, approximately 6 million consisted of geological unit boundary changes and approximately 111 million consisted of physical rock property changes. Statistical measures used for this study include the probability threshold, which records the lithology assigned to a voxel in at least 99% of the acceptable models which satisfy the observed magnetic and gravity observations. Additional statistical measures include the mean density and mean susceptibility, which are also derived from the accumulated accepted inversion proposals/models.

The gravity inversion converged first (after approximately 25 million iterations), with the rms misfit stabilizing at approximately 0.3 mGal, close to the noise estimate of the observed data given the model resolution. Multiple small-scale short-wavelength positive and negative features in the residual gravity misfit indicate departures from bulk mean unit properties that may arise from alteration or other processes associated with mineral systems, and thus present targets for exploration follow-up. Edge effects at the eastern boundary of the model may reflect regional de-trending and that padding algorithms are not entirely accounting for sources located just outside the model area. A positive residual was associated with the Catos Creek dyke, suggesting that this granodiorite may be more dense and thus possibly more mafic in composition than had been ascribed.

The magnetic inversion took longer to converge than gravity (approximately 50 million iterations), with the misfit stabilizing at approximately 3 nT. The residual misfit, which was negligible, except for a few voxels with outlier positive residuals, which the model could not account for. These may represent additional volumes of anomalously magnetic (possibly pyrrhotitic) material in the Mathinna Supergroup above and beyond the more magnetic sub-population allowed by the a priori defined bimodal magnetic susceptibility distribution for these units. The most prominent instance of this (~2 km east of center) is the North Scamander

Pb-Cu-Ag-Zn prospect, where massive magnetite (up to 40% by volume) has been intersected by drilling at a DDH depth of ~200 metres. More moderately magnetic inversion voxels shown at 599900E and 602000E on the 5413500N east-west cross-section correspond, respectively, to disseminated and vein magnetite drilled at depth in the Great Pyramid Sn deposit (DH SPG1A, with highly variable susceptibilities, (Duffett, 1992), and a magnetic anomaly extending over 1.5 km NNW, where disseminated pyrrhotite has been intersected by drilling (CR DH1).

With regard to the Great Pyramid tin deposit, the inversion placed, with high probability, a less voluminous granite. Depth to the top of the prominent cupola remains at approximately 400 metres (beneath that of the deepest drilling to date at Great Pyramid, 348 metres), suggestive of being the source of mineralizing hydrothermal fluids responsible for the Great Pyramid deposit. The North Scamander and Orieco copper deposits are also proximal to nearby granite cupolas, supporting the granite's role in their genesis. Overall, the inversion result supports the hypothesis of granite-derived fluids as the most likely source of metals, with the temperature of the fluid and distance from granite controlling the mineralogy of the deposits in the Scamander Mineral Field. The emergence of granite roots extending some kilometers downwards is a more questionable outcome of the inversion, possibly indicating overfitting of the gravity data or insufficient density contrast with the underlying basement material. A high degree of uncertainty is placed at the boundary between Devonian Granite and Mathinna lithologies. High levels of uncertainty are also associated with the geometry of the Scamander Tier Dyke, which the inversion renders less voluminous than in the reference model. This is attributable to the low-density contrast between Mathinna Supergroup meta-turbidites and the granodiorite dyke (Bombardieri et al., 2021)

#### 4.0 REFERENCES

- Bombardieri, D., Duffett, M., McNeill, A., Vicary, M., Paterson, R. 2020. 3D Geophysical modeling of the Alberton-Mathinna section of the “Main Slide”, Northeast Tasmania. *Interpretation*, 8, T525–T540.
- Bombardieri, D., Duffett, M., McNeill, A., Cracknell, M., Reading, A. 2021. Insights and Lessons from 3D Geological and Geophysical Modeling of Mineralized Terranes in Tasmania. *Minerals*, 11(11):1195. <https://doi.org/10.3390/min11111195>
- Black, L. P., Everard, J. L., McClenaghan, M. P., Korsch, R. J., Calver, C. R., Fioretti, A. M., Brown, A. V., Foudoulis, C. 2010. Controls on Devonian–Carboniferous magmatism in Tasmania, based on inherited zircon age patterns, Sr, Nd and Pb isotopes, and major and trace element geochemistry. *Australian Journal of Earth Sciences*, 57, 933–968.
- Duffett, M. L. 1992. *Geophysics of the Scamander Mineral Field*. Bachelor’s (Hons) Thesis, The University of Tasmania, Hobart, Australia.
- Drummond, A., Lake, T. 2014. Retention Licence 2/2009 GREAT PYRAMID ANNUAL REPORT TO 01 AUGUST 2014. TNT Mines Limited. MRT Company Report 16\_7586 (unpubl.) URL [http://mrttomcatpw.dept.prod/mrtdoc/tasxplor/download/16\\_7586/RL2\\_2009\\_AR\\_to\\_01\\_Aug\\_2014.pdf](http://mrttomcatpw.dept.prod/mrtdoc/tasxplor/download/16_7586/RL2_2009_AR_to_01_Aug_2014.pdf)
- Fullagar, P., Pears, G. and McMonnies, B. 2008. Constrained inversion of geological surfaces - pushing the boundaries. *The Leading Edge*, 27, No. 1, 98–105.
- Groves, D. I. 1972. The zoned Mineral Deposits of the Scamander-St Helens District. Bulletin of the Geological Survey of Tasmania, *Geological Survey Bulletin*, 53, URL <https://www.mrt.tas.gov.au/mrtdoc/dominfo/download/GSB53/GSB53.pdf>
- Leaman, D. E. 2012. An interpretation of the granitoid rocks of eastern Tasmania. Mineral Resources Tasmania GPCR2012\_01.
- McInerney, P., Lane, R., Seikel, R., Guillen, A., Gibson, H. and FitzGerald, D. 2013. *Forward modelling and inversion with 3D GeoModeller*. Intrepid Geophysics, Brighton, Victoria. 162 pages. [http://www.intrepid-geophysics.com/ig/uploads/manuals/documentation\\_pdf\\_geomodeller/pdf\\_en/GeoModeller\\_Forward\\_Modelling\\_Inversion.pdf](http://www.intrepid-geophysics.com/ig/uploads/manuals/documentation_pdf_geomodeller/pdf_en/GeoModeller_Forward_Modelling_Inversion.pdf) (accessed 24 July 2018).
- Ruxton, P., Plummer, G. 1984. Economic geology and fluid inclusion history of the Scamander Mineral Field and Great Pyramid tin deposit, NE Tasmania. In: *Mineral Exploration and Tectonic Processes in Tasmania*, Baillie, P. W., Collins, P. L. F., Eds. Geological Society of Australia, Tasmanian Division: Hobart, Australia.
- Worthing, M. A. and Woolward, I. R. 2010. Explanatory Report for the Dublin Town (5840), *Brilliant* (5841), *Falmouth* (6040) and *Beaumaris* (6041) Geological Map Sheets, 1:25 000 Scale Digital Geological Map Series Explanatory Report, URL [https://www.mrt.tas.gov.au/mrtdoc/dominfo/download/ER25\\_3/ER25\\_3.pdf](https://www.mrt.tas.gov.au/mrtdoc/dominfo/download/ER25_3/ER25_3.pdf)





Tasmanian  
Government

**Mineral Resources Tasmania**

PO Box 56 Rosny Park  
Tasmania Australia 7018  
Ph: +61 3 6165 4800

[info@mrt.tas.gov.au](mailto:info@mrt.tas.gov.au)    [www.mrt.tas.gov.au](http://www.mrt.tas.gov.au)